

## Dynamic Properties of "Hard" Magnetic Bubbles

G. P. Vella-Coleiro, A. Rosencwaig, and W. J. Tabor  
*Bell Laboratories, Murray Hill, New Jersey 07974*  
 (Received 24 July 1972)

A theory is developed to explain the anomalous dynamic behavior of a new type of cylindrical magnetic domain called a hard bubble. This theory, which is based on the Landau-Lifshitz-Gilbert equation of motion, is able to explain satisfactorily all the salient features of the motion of hard bubbles.

A new type of cylindrical magnetic domain, called a hard bubble, has recently been described by Tabor *et al.*<sup>1</sup> The static properties of these bubbles can be explained in terms of a model<sup>2</sup> in which the wall of the bubble is assumed to have several Bloch-to-Néel transitions (Bloch lines). In this paper we consider the implications of this model with regard to the dynamic behavior of hard bubbles. The salient features of the dynamics of hard bubbles are the following<sup>1,3</sup>: (a) Hard bubbles have a component of velocity  $V_{\perp}$  perpendicular to an applied magnetic field gradient as well as a component  $V_{\parallel}$  parallel to the field gradient; (b) the ratio  $V_{\perp}/V_{\parallel}$  becomes large at large values of the drive field; (c) the ratio of  $V_{\parallel}$  to the drive field becomes very small at large values of the drive field. All these features are explained satisfactorily by the theory developed here.

We consider first a planar 180° wall which contains closely spaced Bloch lines as shown in Fig. 1, where the wall lies in the  $y$ - $z$  plane ( $0 \leq \theta \leq \pi$ ). We adopt the linear model of Rosencwaig, Tabor, and Nelson,<sup>2</sup> where the angle  $\psi$  is assumed to be a linear function of  $y$  for the stationary wall. However, for a wall in motion the spin configuration is not necessarily linear. In either case, for closely spaced Bloch lines the additional wall energy density consists mainly of the exchange energy  $A(\partial\psi/\partial y)^2$  ( $A$  is the exchange constant), and so we ignore all other contributions. Thus, the only significant  $\theta$  component of the torque acting on the spins is the exchange torque  $-2A\partial^2\psi/\partial y^2$ .

The Landau-Lifshitz-Gilbert equation of motion of the spins can be written in component form as follows<sup>4</sup>:

$$\dot{\theta} = -T_{\theta}\gamma/M - \alpha \sin\theta\dot{\psi}, \quad (1)$$

$$\dot{\psi} \sin\theta = -T_{\psi}\gamma/M + \alpha\dot{\theta}, \quad (2)$$

where  $T_{\theta}$  and  $T_{\psi}$  are the  $\theta$  and  $\psi$  components of the torque, respectively,  $\gamma$  ( $>0$ ) is the gyromagnetic ratio,  $M$  is the saturation magnetization,

and  $\alpha$  is the damping constant.  $\dot{\theta}$  and  $\dot{\psi}$  can be written in terms of the  $x$  and  $y$  components of the wall velocity,  $v_x$  and  $v_y$ , as follows:

$$\dot{\theta} = v_x \partial\theta/\partial x, \quad \dot{\psi} = v_y \partial\psi/\partial y,$$

where we have set  $\partial\theta/\partial y = \partial\psi/\partial x = 0$  for a wall moving with constant velocity. Since Eqs. (1) and (2) are valid at every point in the wall, the wall velocity can be obtained by solving these equations at some point in the wall without loss of generality. It is convenient to solve the equations at the wall center ( $\theta = \pi/2$ ) where we have

$$\partial\theta/\partial x = \pi/l_w, \quad T_{\psi} = MH,$$

where the first equation serves as a definition of the dynamic wall width  $l_w$ , and  $H$  is an external magnetic field in the  $-z$  direction. (In the following we shall ignore the difference between the dynamic and static wall widths since this difference is small at small velocities.) Hence, Eqs.

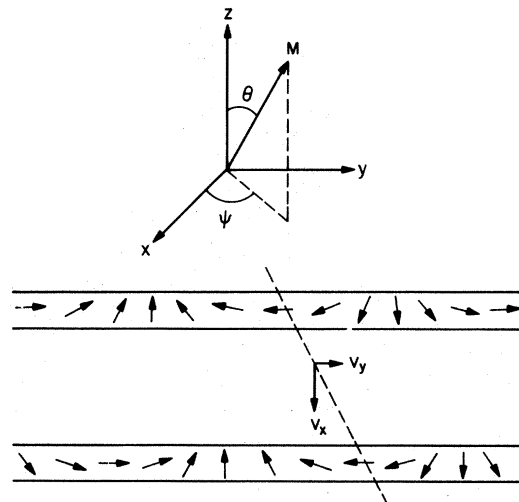


FIG. 1. The coordinate system used to describe a planar 180° wall with Bloch lines. The wall lies in the  $y$ - $z$  plane and  $0 \leq \theta \leq \pi$ .

(1) and (2) become, at  $\theta = \pi/2$ ,

$$v_x \frac{\pi}{l_w} = \frac{2\gamma A}{M} \frac{\partial^2 \psi}{\partial y^2} - \alpha v_y \frac{\partial \psi}{\partial y}, \quad (3)$$

$$v_y \frac{\partial \psi}{\partial y} = -\gamma H + \alpha v_x \frac{\pi}{l_w}. \quad (4)$$

For the stationary wall ( $H=0$ ) we have assumed  $\partial^2 \psi / \partial y^2 = 0$ . When  $H \neq 0$ ,  $\partial^2 \psi / \partial y^2$  is still zero if the spins are free to precess, as shown in Fig. 1. In this case we can solve Eqs. (3) and (4) to obtain<sup>5</sup>

$$\mu_x = \frac{v_x}{H} = \frac{\gamma \alpha}{1 + \alpha^2} \frac{l_w}{\pi}, \quad (5)$$

$$\mu_y = \frac{v_y}{H} = \pm \frac{\gamma}{1 + \alpha^2} \frac{1}{2\pi\rho}, \quad (6)$$

where  $\rho = |\partial \psi / \partial y| / 2\pi$  is the number of Bloch lines per unit wall length (a Bloch line involves a spin rotation of  $2\pi$  rad) and the plus or minus sign stands for clockwise or counterclockwise rotation of the spin direction through the Bloch line. It is thus evident that the Bloch lines have a tangential component of velocity as well as a perpendicular component. This fact can be seen pictorially by following the path of the center of a Bloch line as shown in Fig. 1. The direction of the tangential component of velocity depends on the direction of rotation of the spin direction in the Bloch line. It is also to be noted that the mobility  $\mu_x$  normal to the wall given by Eq. (5) differs from the mobility of a normal wall by the factor  $\alpha^2 / (1 + \alpha^2)$ . For low damping materials  $\alpha \ll 1$ , and the wall with Bloch lines has a much smaller mobility than a normal wall.

In the model of Rosencwaig, Tabor, and Nelson,<sup>2</sup> the wall of a hard bubble is assumed to be of the type discussed above. Hence, when a field gradient  $H = H_0 \sin \eta$  is applied to a hard bubble, the torque acting on the spins produces an increase in the density of Bloch lines on one side of the bubble and a reduction on the other side, the total number of Bloch lines remaining unchanged (see Fig. 2). Thus  $\partial^2 \psi / \partial y^2$  is no longer equal to zero. To estimate the effect of  $\partial^2 \psi / \partial y^2 \neq 0$  let us first consider the case where the wall is constrained to move with  $v_y = 0$ , i.e., the Bloch lines are prevented from having a tangential component of velocity. In this case the solution of Eqs. (3) and (4) becomes

$$\mu_x = v_x / H = (\gamma / \alpha) (l_w / \pi), \quad (7)$$

$$\partial^2 \psi / \partial y^2 = MH / 2A\alpha. \quad (8)$$

If  $v_y$  is not zero, but has a value smaller than

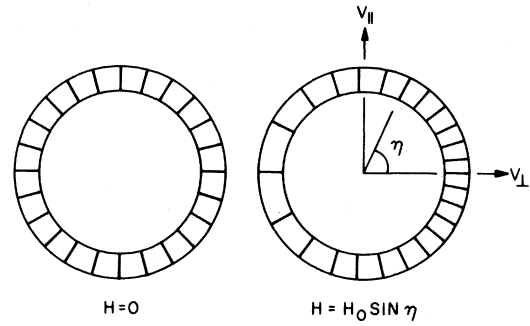


FIG. 2. Distribution of Bloch lines in a hard bubble with and without an applied magnetic field gradient. The radial bars represent the centers of the Bloch lines.

that given by Eq. (6), the value of  $\partial^2 \psi / \partial y^2$  will lie between zero and the value given by Eq. (8). This situation occurs for the wall of a hard bubble in a field gradient  $H = H_0 \sin \eta$ , and so we write

$$\partial^2 \psi / \partial y^2 = (MH_0 / 2A\alpha) f \sin \eta, \quad (9)$$

where  $y = \eta d / 2$  and  $d$  is the bubble diameter. On integrating we obtain

$$\partial \psi / \partial y = \pm 2n_0 / d - (MH_0 d / 4A\alpha) f \cos \eta, \quad (10)$$

where  $n_0$  is the total number of Bloch lines in the bubble and  $0 \leq f \leq 1$ , and we make the reasonable assumption that  $f$  is a monotonically increasing function of  $n_0$  and of the amplitude  $H_0$  of the field gradient. Hence, the number of Bloch lines per unit length of bubble wall is

$$\rho = n_0 / \pi d \pm (MH_0 d / 8\pi A\alpha) f \cos \eta, \quad (11)$$

i.e., the density of Bloch lines is larger on one side of the bubble than it is on the opposite side. Since we have made the assumption that the Bloch lines are closely spaced, the theory developed here cannot be applied when  $H_0$  is large enough to cause  $\rho$  to become small in any region of the bubble wall.

The wall width derived by Rosencwaig, Tabor, and Nelson,<sup>2</sup> in the limit where the exchange energy is much larger than the anisotropy and demagnetizing field energies, can be written as

$$l_w / \pi = (\sqrt{2\pi\rho})^{-1}. \quad (12)$$

On solving Eqs. (3) and (4) with the values given by Eqs. (9)-(12), we obtain

$$\mu_x = \frac{v_x}{H} = \frac{\gamma(\alpha^2 + f)}{\alpha(1 + \alpha^2)} \frac{1}{\sqrt{2\pi\rho}}, \quad (13)$$

$$\mu_y = \frac{v_y}{H} = \pm \frac{\gamma(1 - f)}{1 + \alpha^2} \frac{1}{2\pi\rho}, \quad (14)$$

TABLE I. Comparison between measured and calculated velocities of hard bubbles.

<i>d</i> (μm)	$\Delta H$ (Oe)	$V_{\parallel}/\Delta H$ (cm/sec Oe)		$V_{\perp}/\Delta H$ (cm/sec Oe)		$V_{\perp}/V_{\parallel}$		<i>f</i>
		Meas	Calc	Meas	Calc	Meas	Calc	
6.2	0.8	15.0	15.7	32.5	34.5	2.2	2.2	0.21
6.2	2.5	5.0	5.0	29.1	29.1	5.8	5.8	0.43
6.2	5.9	2.8	2.7	24.4	23.9	8.8	8.8	0.54
3.9	0.3	27.7	12.4	45.0	20.2	1.6	1.6	0.16
3.9	1.4	8.4	7.4	24.9	21.7	2.9	2.9	0.27
3.9	3.5	3.0	2.3	21.6	16.8	7.2	7.2	0.48
3.3	3.0	4.2	5.1	14.7	17.9	3.5	3.5	0.31

where both  $\mu_x$  and  $\mu_y$  are functions of  $\eta$  through the term  $\rho$ .

In order to relate the wall velocities  $v_x, v_y$  to the bubble velocities  $V_{\parallel}, V_{\perp}$  (Fig. 2), we assume that the bubble can move without significant distortion. On equating the total component of the external pressure acting on the bubble wall in the direction of  $V_{\parallel}$  to the total component of the internal pressure in the same direction, and similarly for the direction of  $V_{\perp}$ , we have

$$\int_0^{2\pi} 2M(v_x/\mu_x + v_y/\mu_y) \sin\eta \, d\eta = \int_0^{2\pi} 2M(V_{\parallel}/\mu_x - V_{\perp}/\mu_y) \sin^2\eta \, d\eta = \int_0^{2\pi} 2MH_0 \sin^2\eta \, d\eta,$$

$$\int_0^{2\pi} 2M(v_x/\mu_x + v_y/\mu_y) \cos\eta \, d\eta = \int_0^{2\pi} 2M(V_{\perp}/\mu_x + V_{\parallel}/\mu_y) \cos^2\eta \, d\eta = 0,$$

where the contributions from the two velocity components have been added since they both produce damping (damping constant =  $2M/\mu$ ) of the wall motion. After integrating we obtain

$$\frac{V_{\perp}}{V_{\parallel}} = \mp \sqrt{2} \frac{(\alpha^2 + f)}{\alpha(1 - f)}, \tag{15}$$

$$\frac{V_{\parallel}}{\Delta H} = \frac{d}{4n_0} \frac{\gamma}{(1 + \alpha^2)} F, \tag{16}$$

where  $\Delta H = 2H_0$  is the field difference across the bubble and

$$F = \left( \frac{\alpha}{\sqrt{2}(\alpha^2 + f)} + \frac{\sqrt{2}(\alpha^2 + f)}{\alpha(1 - f)^2} \right)^{-1}.$$

A typical value of the Landau-Lifshitz damping parameter  $\lambda/\gamma^2$  for a high-mobility garnet is<sup>6</sup>  $1.4 \times 10^{-7}$  Oe<sup>2</sup> sec/rad. Hence, we have  $\alpha = \lambda/\gamma M = 0.2$ , using the values  $\gamma = 1.76 \times 10^7$  rad sec<sup>-1</sup> Oe<sup>-1</sup> and  $4\pi M = 150$  G.  $V_{\parallel}/\Delta H$ ,  $V_{\perp}/\Delta H$ , and  $V_{\perp}/V_{\parallel}$  are plotted versus  $f$  in Fig. 3 with these values of the parameters and  $d = 6.2 \mu\text{m}$  and  $n_0 = 50$ , which is a typical value for  $n_0$  for hard bubbles in this material (Rosenzweig, Tabor, and Nelson<sup>2</sup>). A direct comparison can thus be made with the measured values reported in Ref. 1 which are reproduced in Table I (the values of  $\Delta H$  shown are the values of the drive field in excess of the minimum value required to make the bubble just move).

In order to compare the measured velocities

with the theory, we have obtained values of  $f$  from Eq. (15) using the measured values of  $V_{\perp}/V_{\parallel}$  shown in Table I. Using these values of  $f$  we then calculated the values of  $V_{\parallel}/\Delta H$  and  $V_{\perp}/\Delta H$ . Both of these are included in Table I, although only one is independent once the ratio  $V_{\perp}/V_{\parallel}$  is specified. It can be seen from Table I that the agreement between theory and experiment is very good.

The theory developed above is thus able to explain the dynamic behavior of hard bubbles using

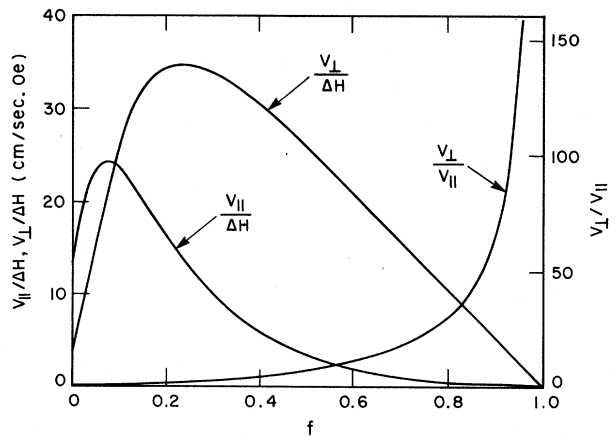


FIG. 3.  $V_{\parallel}/\Delta H$ ,  $V_{\perp}/\Delta H$ , and  $V_{\perp}/V_{\parallel}$  versus  $f$  for the following parameter values:  $d = 6.2 \mu\text{m}$ ,  $n_0 = 50$ ,  $\alpha = 0.2$ ,  $\gamma = 1.76 \times 10^7$  rad sec<sup>-1</sup> Oe<sup>-1</sup>.

the same model which was developed to explain the static properties. The velocity component perpendicular to the applied field gradient follows naturally from the Landau-Lifshitz-Gilbert equation of motion without the introduction of any arbitrary assumptions. The dependence of the bubble velocity components on the drive field is correctly explained qualitatively by the introduction of the  $f$  factor, but a quantitative comparison with experiment must await a detailed derivation of the dependence of  $f$  on the drive field.

<sup>1</sup>W. J. Tabor, A. H. Bobeck, G. P. Vella-Coleiro, and

A. Rosencwaig, *Bell Syst. Tech. J.* **51**, 1427 (1972).

<sup>2</sup>A. Rosencwaig, W. J. Tabor, and T. J. Nelson, preceding Letter [*Phys. Rev. Lett.* **28**, 946 (1972)]. A similar although incomplete model has been proposed independently by A. P. Malozemoff, *Appl. Phys. Lett.* **21**, 149 (1972).

<sup>3</sup>Anomalous motion of bubbles in a field gradient has also been noted recently by J. A. Cape, *J. Appl. Phys.* **43**, 3551 (1972).

<sup>4</sup>J. C. Slonczewski, *Int. J. Magn.* **2**, 85 (1972).

<sup>5</sup>Expressions similar to our Eqs. (5) and (6) have been obtained independently in connection with the collapse dynamics of hard bubbles by A. P. Malozemoff and J. C. Slonczewski, following Letter [*Phys. Rev. Lett.* **28**, 952 (1972)].

<sup>6</sup>G. P. Vella-Coleiro, D. H. Smith, and L. G. Van Uitert, *Appl. Phys. Lett.* **21**, 36 (1972).

## Effect of Bloch Lines on Magnetic Domain-Wall Mobility\*

A. P. Malozemoff and J. C. Slonczewski

*IBM Thomas J. Watson Research Center, Yorktown Heights, New York 10598*

(Received 2 August 1972)

Certain magnetic domain walls in a garnet film show a much reduced mobility from that of normal domain walls in the film and are interpreted to contain vertical Bloch lines. Theory shows that forward wall motion involves sideways propagation of Bloch lines and that in the high Bloch-line density limit, the mobility for small  $\alpha$  is reduced to  $\alpha^2$  of the conventional value, where  $\alpha$  is the Gilbert damping parameter.

Until recently the theory of ferromagnetic or ferrimagnetic domain wall motion in a constant field has been confined to the case of a uniform Bloch wall propagating in an infinite medium. It has therefore involved only one-dimensional solutions of the Landau-Lifshitz equation. In this case, Döring<sup>1</sup> has shown that the velocity of the wall is governed by the precession of the magnetization within the wall width about the demagnetizing field of the wall, and Walker<sup>2</sup> has calculated an upper limit of this velocity. More recently, the theory has been extended by Slonczewski<sup>3,4</sup> and by Schlömann<sup>5</sup> to cases of thin films where two-dimensional solutions are required because surface stray fields vary along the thickness of the film. In one of these cases, interacting of a horizontal (parallel to film plane) Bloch line with the stray field was invoked to account for critical-velocity observations of Argyle, Slonczewski, and Mayadas.<sup>4</sup>

In this paper we consider a new kind of wall motion involving the propagation of Bloch lines. We have studied such effects experimentally in garnet films with anomalous cylinder (bubble) and stripe

domains. The static behavior of these domains has been interpreted in a previous paper<sup>6</sup> (I), and also by Tabor *et al.*,<sup>7</sup> in terms of vertical (parallel to easy axis) Bloch lines interacting along the perimeter of the domain. We will argue that the mobility of such walls is a two-dimensional problem, involving forward propagation of the wall and sideways propagation of Bloch lines.<sup>8</sup> However, in contrast to the earlier studies in films,<sup>3,5</sup> the surface of the specimen plays no essential role in the dynamic phenomenon, which should therefore occur as well in a bulk specimen, given the initial presence of Bloch lines.

In I, a garnet film 7  $\mu\text{m}$  thick and of composition  $(\text{Yb}_{0.15}\text{Eu}_{0.85}\text{Y}_{2.2})(\text{Ga}_{1.1}\text{Fe}_{3.9})\text{O}_{12}$  was shown to sustain classes of bubbles and stripes with different characteristic dependences of dimensions on field and different characteristic collapse fields. We chose to study the mobility of the bubbles with the highest collapse field (132 Oe in Fig. 2 of I) because we could easily differentiate them from other bubbles by lifting the bias field to just under this collapse field and thus eliminating all other bubbles and stripes. We measured